Published in final edited form as:
Ophthalmology. 2011 August ; 118(8): 1571–1579. doi:10.1016/j.ophtha.2011.01.016.

Choroidal Thickness Measured by Spectral Domain Optical Coherence Tomography: Factors Affecting Thickness in Glaucoma Patients

Eugenio A. Maul, MD[1], **David S. Friedman, MD, PhD**[1], **Dolly S. Chang, MD**[1], **Michael V. Boland, MD, PhD**[1], **Pradeep Y. Ramulu, MD, PhD**[1], **Henry D. Jampel, MD, MHS**[1], and **Harry A. Quigley, MD**[1]

[1]The Glaucoma Service and Dana Center for Preventive Ophthalmology, The Wilmer Eye Institute at Johns Hopkins University

Abstract

Purpose—To measure choroidal thickness and to determine parameters associated with it.

Design—Cross-sectional study.

Participants—Seventy-four glaucoma patients and glaucoma suspects.

Methods—Spectral domain optical coherence tomography (SDOCT) scans were obtained to estimate average choroidal thickness in a group of glaucoma suspects and glaucoma patients. Average thickness was calculated from enhanced depth SDOCT images and manually analyzed with Image J software. Open angle glaucoma, open angle glaucoma suspect, primary angle closure glaucoma, primary angle closure, and primary angle closure suspect were defined by published criteria. Glaucoma suspects had normal visual fields bilaterally. Glaucoma was defined by specific criteria for optic disc damage and visual field loss in at least one eye. The most affected eye was analyzed for comparisons across individuals, while right/left and upper half/lower half comparisons were made to compare thickness against degree of visual field damage.

Main Outcome Measured—Average macular and peripapillary choroidal thickness measured using SDOCT.

Results—The choroidal-scleral interface (CSI) was visualized in 86% and 96% of the macular and peripapillary scans, respectively. In multivariable linear regression analysis, the macular choroid was significantly thinner in association with 4 features: longer eyes (22 μm per mm longer [95% confidence Interval (CI): −33, −11]), older individuals (31 μm thinner per decade older [95% CI: −44 −17]), lower diastolic ocular perfusion pressure (26 μm thinner per 10 mmHg lower [95% CI: 8, 44]), and thicker central corneas (6 μm per 10 μm thicker cornea [95% CI: −10, 0]). The choroid was not significantly thinner in glaucoma patients than in suspects (14 μm [95% CI:

Correspondence: Eugenio A. Maul MD, Wilmer 125, Johns Hopkins Hospital, 600 N.Wolfe St., Baltimore, MD 21287. Telephone: (+1) 443-955-6052, Fax: (+1) 410-955-1985, emaul@jhsph.edu.

Presented in part at the Association for Vision and Research in Ophthalmology Annual Meeting, May 2010.

Financial Disclosures: Dr Quigley receives financial (research) support from Alcon, Heidelberg Engineering and the NIH-NEI. Dr Friedman receives financial (research) support from Carl Zeiss Meditec. Dr Jampel is a paid consultant of Endo-Optics, Ivantis, Transcend and Mobius; and is also equity owner for Allergan. No conflicting relationship exists for any other authors.

−54, 26], p=0.5). Peripapillary choroidal thickness was not significantly different between glaucomaand suspect patients. Thickness was not associated with damage severity as estimated by visual field mean deviation or nerve fiber layer thickness, including comparisons of right to left eye or upper to lower values.

Conclusion—Age, axial length, central corneal thickness, and diastolic ocular perfusion pressure are significantly associated with choroidal thickness in glaucoma suspects and glaucoma patients. Degree of glaucoma damage was not consistently associated with choroidal thickness.

Introduction

The choroid is known to have an important role in ocular nutrition, volume regulation, and temperature control.1 The achievement of emmetropia is now known to be dependent upon active mechanisms that sense image blur, move the retina to reduce the blur, and permanently alter ocular dimensions to maintain clear imagery. It is active increase or decrease in choroidal thickness that moves the retina to the correct position, as shown in laboratory investigations in chickens and mammals.2⁻4 Recently, it was demonstrated that similar changes in choroidal thickness occur in humans in response to short-term unilateral image blur.5 Abnormal choroidal thickness increase has been hypothesized to be a contributing feature to primary angle closure (PAC)6, and qualitative increases in choroidal extravascular volume have been confirmed in many PAC and primary angle closure glaucoma (PACG) eyes.7, 8 It is not yet clear whether the normal choroidal thickness regulatory mechanism(s) and those operative in PAC are the same or different.

Abnormalities in choroidal structure and function are likely to contribute to major ocular diseases. Choroidal pathology is central to age-related macular degeneration.9 In addition, it has been hypothesized that abnormal choroidal blood supply10, 11 is one factor in optic nerve damage in open angle glaucoma (OAG). *Post mortem* histological studies have reported the choroid to be thinner in glaucoma12⁻14, but it is unclear whether this finding represents a risk factor or a consequence of the disease. Furthermore, histology is unlikely to represent the thickness of the living choroid, which consists so prominently of blood vessels. Indeed, *in vivo* ultra high resolution optical coherence tomography (UHR-OCT) of porcine choroid compared to the histological appearance of the same eyes illustrates the failure of histological measurements to reflect choroidal thickness accurately15.

The development of methods to measure choroidal thickness *in vivo* has enabled new directions in research into normal and pathological processes in the choroid. Techniques such as partial coherence interferometry and spectral domain optical coherence tomography (SDOCT)16⁻18 permit measurements of the living choroid. Spaide and colleagues have recently modified the acquisition of SDOCT data to improve choroidal visualization.19 Their work has shown that choroidal thickness decreases with age and that the choroid is thinner in eyes with longer axial length.20⁻24 At present, there are still a number of challenges in determining the boundaries of the choroid in SDOCT images and in specifying how best to characterize the structure of the choroid *in vivo*.

We acquired SDOCT images of the choroid in patients in a glaucoma clinic to test methods for measurement of choroidal thickness, to determine biometric features that are related to its thickness, and to perform initial comparisons among glaucoma suspects and glaucoma patients.

Methods

Subjects were selected as a convenience sample of those from a tertiary referral practice of glaucoma who gave verbal informed consent and agreed to the additional testing at times

when staff members were available to test them. The study followed the tenets of the Declaration of Helsinki and was approved by the Johns Hopkins Joint Committee for Clinical Investigation. Adherence to Health Insurance Portability and Accountability Act (HIPAA) guidelines was maintained throughout the study. Eligible subjects were over 18 years old, had visual acuity of 20/40 or better, had clear ocular media, had undergone at least 1 reliable visual field test (with fixation losses, false negatives and false positives all < 33%), and were diagnosed as primary angle closure suspect (PACS), primary angle closure (PAC), primary angle closure glaucoma (PACG), open angle glaucoma suspect (OAGS) or open angle glaucoma (OAG). Exclusion criteria included any retinal or neuro-ophthalmological disease, amblyopia, intraocular surgery during the previous 6 months, secondary glaucoma and active, chronic or recurrent uveitis. Diagnoses were based on criteria by Foster et al25 and applied by one of us (HQ).

The examination protocol was conducted in a seated, resting position and included measurement of blood pressure and heart rate, axial length and keratometry in both eyes using the IOL Master (Carl Zeiss Meditec, Dublin, CA.), followed by SDOCT scans of the macular and peripapillary regions using the Heidelberg Spectralis (Heidelberg Instruments, Inc., Heidelberg, Germany). Scans were attempted in both eyes of every recruited patient, with random assignment for the first eye scanned and the first region scanned (macular or peripapillary) to prevent potential bias in bilateral comparisons.

SDOCT images were obtained by Enhanced Depth Imaging, a method that improves resolution of choroidal detail when focus is manually placed more posteriorly than in standard retinal SDOCT images which results in the production of inverted images.19 The macular region was scanned using a single 30 degree linear scan centered on the fovea. The peripapillary region was scanned using a circular scan 12 degrees in diameter, centered on the optic disc. (Figure 1a) Two scans were obtained in both regions and the image with the best visualization of the border between the choroid and sclera, the choroidal-scleral interface (CSI), was used. If neither of the two images had a clearly identifiable CSI, additional images were taken to produce the best possible view of the CSI. Keratometry readings and the most recent refraction were entered into the Heidelberg Explorer Software to estimate optical magnification and, therefore, to allow for more accurate comparisons across individuals. By comparing image measurements of patients in the study with and without keratometry/refraction data, we determined that average choroidal thickness would have been different by > 5% in 41% (30/74) of the selected images and by > 10% in 9% (7/74) if we had not accounted for magnification.

One image centered on the fovea (macular choroid) and one centered on the optic disc (peripapillary choroid) were selected for each eligible eye. All selected images, as well as the scaling factor correcting for magnification, were de-identified and exported from the SDOCT. Images were then rescaled to a unified scale, overlaid with a grid indicating the length of the sectors to be measured, and finally measured using ImageJ software (NIH, Bethesda). The choroid was manually outlined, with the anterior border at the basal aspect of retinal pigment epithelium (RPE), which is a clear boundary in nearly every image (Figure 1b–c). The posterior boundary, or CSI, is more variable among images. In the majority of images, there was a hyper-reflective line between the large vessel layer of the choroid and the sclera (Figure 2), which we marked as the CSI. When the image contained a CSI that appeared well delineated and thinner than the RPE it was graded as "good", but if the CSI appeared thicker than the RPE, the CSI was marked reproducing the RPE's thickness; these were classified as "fair" images (Figure 2c–d). Finally, in a few images (classified as "poor"), there was no clear boundary for the CSI; in these, the posterior choroid was marked as a smooth line joining the outer limits of the large choroidal vascular

spaces (Figure 2e–f). This approach for the poorer images may fail to include some extravascular choroid.

Once the anterior and posterior boundaries were marked, the area occupied by the choroid over a 6mm long segment was measured and used to calculate the average choroidal thickness (Figure 1). For the macular choroid, this area was centered on the fovea, extending 3 mm in either side. For the peripapillary choroid, the circular area, 12 degrees in diameter, was represented as a linear strip. The overall 360° peripapillary average thickness and well as the superior and inferior 180° average thickness were calculated. In addition to the Enhanced Depth Images of the choroid, peripapillary nerve fiber layer (NFL) thickness was measured from Spectralis images in the standard focus setting.

The primary analysis compared the average macular choroidal thickness, then the peripapillary choroidal thickness across subjects. We selected for this analysis the eye of each subject with the most negative mean deviation (MD) in its visual field test. Independent variables that were compared to each choroidal thickness zone in both univariable and multivariable analysis included: glaucoma diagnosis, age, race, sex, axial length, both the highest intraocular pressure (IOP) recorded in chart and IOP on the day of imaging, central corneal thickness (CCT), visual field MD, history of previous glaucoma surgery, phakic status, number of glaucoma medications being used, heart rate, systolic blood pressure (SBP), diastolic blood pressure (DBP), and ocular perfusion pressures: systolic, diastolic and mean. Systolic perfusion pressure was calculated as the difference between SBP and IOP, diastolic perfusion pressure was the difference between DBP and IOP, and mean ocular perfusion pressure was calculated as the difference between mean blood pressure and IOP. Mean blood pressure was calculated using the following formula: Mean BP = DBP + (1/3*[SBP-DBP]). The multivariable regression models were fitted with inclusion of age, sex, race and glaucoma diagnosis in each model. The remaining variables were selected using a backwards stepwise approach with significance set at 5%. Model goodness of fit was assessed using Akaike information criteria.26 Statistical analyses were conducted using Stata 11.0 (Stata Corporation, College Station, TX).

Additional analyses were conducted in glaucoma patients (those meeting the field loss criteria) to determine if there was a relationship between degree of damage and choroidal thickness. First, we compared macular choroidal thickness between the right and left eye in those subjects with both eyes eligible. Then, we divided the peripapillary choroidal thickness data into superior and inferior hemispheres and compared these to the MD in visual field tests for the correspondingly opposite hemifield. We calculated the MD for the superior and inferior hemifields by averaging the pointwise total deviation values in each region.

The projected sample size to detect a 20% (approximately 50 μm) difference between glaucoma and suspect eyes with a significance of 5% and a power of 80%, assuming a standard deviation of 76 μm24, was estimated to be 36 patients per group. A set of 60 macular and 60 peripapillary images were randomly selected and traced by two graders masked to diagnosis and to each other’s grading. The intraclass correlation coefficients for average macular choroidal thickness as well as overall peripapillary choroidal thickness were used to assess agreement between both graders.

Results

Seventy-four patients, 37 with glaucoma and 37 glaucoma suspects, met the eligibility criteria between October, 2009 and February, 2010. SDOCT macular scans were obtained at least one eye in 73/74 subjects, and in at least one eye in 73/74 subjects for the peripapillary

scans. Intraclass correlation coefficient (95% Confidence Interval [CI]) for the measures obtained by both graders in the 60 re-measured macular and peripapillary scans were 0.97 (0.95–0.98) and 0.98 (0.97–0.99), respectively. Images were graded as having good, fair and poor quality in 33/73, 30/73 and 10/73 macular scans; and 20/73, 51/73 and 2/73 of the peripapillary scans respectively. All images were included in the analysis, whether classified as good, fair or poor. Poor quality macular scans had on average a thicker choroid than fair quality scans (mean se) = 358 (20) μm vs 267 (14) μm, $p<0.001$) and subsequently fair quality macular scans had a significantly thicker choroid than good quality scans (mean (se) = 267 (14) μm vs 195 (11) μm, $p<0.001$). Peripapillary scans did not significantly differ by image grading, but there were only 2 images of poor quality and the choroid was on average thinner than in the macular scans. Average peripapillary choroidal thickness (se) for poor, fair and good images was 330 (45) μm, 189 (10) μm and 163 (13) μm.

The demographic and clinical features of subjects by diagnostic group indicate some significant differences (Table 1). As expected from our diagnostic criteria, glaucoma patients had worse mean deviation and thinner NFL, higher historical IOP levels, and a higher proportion of past trabeculectomy surgery. However, on the day of imaging, IOP level did not differ by group. The small PACG group had the highest proportion of past trabeculectomy.

Image quality did not differ by glaucoma status in either the macular or peripapillary scans. (Fischer's exact test p= 0.65 and p=0.75 respectively).

Variables that were significantly related to thinner macular choroidal thickness in univariable analysis were older age, longer axial length, glaucoma (versus suspect group), and greater NFL loss (Table 2). In a stepwise multivariable model that included glaucoma versus suspect as the diagnostic categorization (Table 3), there were highly significant associations between thinner macular choroid and older age, longer axial length, thicker CCT, and lower diastolic perfusion pressure (all $p < 0.01$). The magnitude of the associations is shown by the following data: older age (30 μm per decade older [95% CI: −44, −16]), longer axial length (26 μm per mm longer [95% CI: −36, −17]), lower diastolic perfusion pressure (30 μm per 10 mmHg lower [95% CI: 11, 49]) and thicker CCT (6 μm per 10 μm thicker cornea [95% CI: −10, −2]). Since IOP is a component of the formula for perfusion pressure, we constructed models with IOP alone, DBP alone, DBP plus IOP, and diastolic perfusion pressure alone as independent variables. The strongest statistical association with choroidal thickness was with diastolic perfusion pressure, for both macular and peripapillary choroid (Table 4). Interestingly, IOP itself was not significantly a factor alone—but by including it in the formula for diastolic perfusion pressure, the significance of blood pressure in the model was enhanced. Interestingly, SBP and systolic perfusion pressure were not significantly associated with choroidal thickness in either univariable or multivariable models.

While glaucoma patients had a macular choroidal thickness that was on average 55 μm thinner than in suspects (20% thinner, p=0.005), this difference was only 14 μm thinner in the multivariable model and did not remain statistically significant (p=0.48). Previous trabeculectomy surgery was associated with a thinner choroid in this model (Table 3, p=0.05). Visual field MD and NFL thickness were not associated with macular choroidal thickness in the multivariable model (Figure 3).

In a second stepwise multivariable model, with the 4 diagnostic groups as a categorical variable (OAGS as reference, and OAG, PAC/S, and PACG), the same 4 parameters were related to thin choroid (older age, long axial length, lower diastolic perfusion pressure and thicker CCT), and the PACG group was the single significant category with thinner choroid

(Table 5). Linear combination of coefficients from the stepwise model (Table 5) revealed that the PACG group had a statistically thinner choroid than the PAC/S (106 μm, p=0.001) and OAGS groups (64 μm, p=0.03), but the difference between PACG and OAG was of borderline significance (49 μm, p=0.07). The difference between OAG and OAG suspects was not significant (p=0.4).

Univariable and multivariable modeling of data for parameters related to peripapillary choroidal thickness were similar to those for macular choroid, including significant thinner choroid with older age, longer eye, and lower diastolic perfusion pressure (Tables 6, 7 and 8, available at http://aaojournal.org). While the magnitude of the coefficients was similar for CCT in the peripapillary analysis, they only reached borderline statistical significance in the multivariable models presented in Tables 7 and 8 (p= 0.06 and p=0.05 respectively).

The choroidal thickness was also measured in a single location immediately underlying the fovea (subfoveal), with comparison to the average macular and peripapillary choroidal thicknesses (Table 9, available at http://aaojournal.org). These data are presented as both crude figures and adjusted for sex, race, age, axial length, central corneal thickness and diastolic perfusion pressure. The subfoveal choroid was 27 μm thicker (95% CI, [19, 35], p<0.001) than the average choroid across the macular zone 3 mm on either side of the fovea. Average macular choroid was 62 μm thicker than the average peripapillary choroid (95% CI, [51, 73], p<0.001), while the subfoveal point thickness was 89 μm thicker than the average peripapillary thickness 95% CI, [73, 105], p<0.001).

To analyze the potential effect of glaucoma damage on choroidal thickness, 25 patients with visual field loss in at least one eye and two eligible eyes were compared for MD and macular choroidal thickness. This included 21 individuals (42 eyes) with OAG and 4 persons (8 eyes) with PACG. There was no significant association between the difference in MD between right and left eyes and the difference in macular choroidal thickness between eyes ($r^2 = 0.03$, p=0.2; Figure 4. We divided peripapillary choroidal thickness into upper and lower halves for 33 eyes of 33 persons with visual field loss and compared the hemi-choroid thickness difference to the hemifield MD difference (contrasting the corresponding halves by inverting the field data). There was no statistically significant correlation (Figure 5).

A sensitivity analysis was conducted censoring images where the CSI was judged to be of poor quality, and the results remained largely unchanged (data not shown). Since image quality of macular scans was associated with a thicker average choroid, we conducted a second sensitivity analysis with image quality included as a covariate. The same predictors remained statistically significant and their coefficients remained of a similar magnitude, except for CCT in the peripapillary choroidal thickness model with detailed diagnosis as a covariate that experienced a shift in the p value form 0.048 to 0.052 while the coefficient remained unchanged (data not shown).

Discussion

Previous investigations of factors associated with choroidal thickness in normal or pseudophakic patients had determined that older persons and eyes with longer axial length or myopic refraction have a thinner choroid.[20–24] Our study has found for the first time that a group of glaucoma suspect and glaucoma patients share these associations. Clearly, the aging process and the axial length are closely related to choroidal thickness as well as being important risk factors for OAG prevalence.[27] Furthermore, we report that eyes with thicker CCT have a thinner choroid, a previously unpublished finding. This extends the many recent reports that link aspects of ocular anatomy and physiology to CCT, including greater risk of OAG incidence.[28] While CCT was significantly associated with choroidal thickness, its

magnitude was smaller than those of other covariates, whose model coefficients remained largely unchanged when CCT was removed from the regression model (data not shown).

In addition, we found a relationship between diastolic perfusion pressure and choroidal thickness. The fact that the choroid was thicker in eyes with higher blood pressure and relatively lower IOP seems logical if the blood volume of the choroid increased with higher diastolic perfusion pressure. While our finding is a cross-sectional comparison among patients, we hypothesize that alterations in blood pressure, IOP, and other parameters will have measureable effects on choroidal thickness. These may be effects on either intravascular volume (as we suggest for blood pressure level) or on extravascular volume. The ability to measure choroidal thickness non-invasively will soon show whether alterations in the choroid play an important role in such events as angle closure glaucoma.6

The present data do not present conclusive evidence that eyes with glaucoma damage differ from glaucoma suspects in choroidal thickness. While glaucoma eyes had significantly thinner macular choroid than suspects, this difference was not significant when adjusted for other parameters in a multivariable model. Furthermore, no association was present for glaucoma eyes compared to suspects in peripapillary choroidal thickness. Specifying type of glaucoma in a multivariable model showed that subjects with PACG had significantly thinner macular (but not peripapillary) choroid than those with OAG, OAGS or PAC/S. We note that our small group of 8 PACG patients had frequently had past trabeculectomy (6/8 eyes), and univariable testing suggested that past glaucoma surgery may influence choroidal thickness. However, choroidal thickness was never significantly different between OAG and OAGS in our data. Consistent with a lack of association between glaucoma damage and choroidal thickness was the failure to find any quantitative correlation between field damage or NFL loss between the two eyes or the upper and lower hemifields of patients with glaucoma.

While we therefore find no strong evidence that glaucoma damage is related to choroidal thickness among suspects and glaucoma patients, we feel that more extensive study is needed to confirm or to refute previous suggestions that glaucoma eyes have a thinner choroid than those with no suspicion of glaucoma—e.g., population-based controls. We are presently engaged in gathering more data along this line. Some previous histological reports suggested that the choroid may be thinner in glaucoma eyes than in non-glaucoma pathology specimens.12⁻14 Yin et al13 found that the choroid was 50 μm thinner in 25 *post mortem* POAG eyes compared to 18 age-matched controls. Kubota et al12 found thinner choroid in 20 enucleated eyes with secondary glaucoma from uveal melanoma compared to 12 enucleated eyes with melanoma and normal IOP. By contrast, Spraul et al29 reported increased choroidal thickness in 20 glaucoma eye-bank eyes compared to 20 age-matched controls. However, histological measures of choroidal thickness in the pig eye do not correlate with their *in vivo* imaging measurements.15 In addition, previous histology studies may not have controlled for the confounding effect of axial length. Even more importantly, our finding that choroidal thickness is influenced by ocular perfusion pressure level means that *post mortem* measurements are even less likely to represent the true state of the tissue.

With the development of new technology for *in vivo* assessment of the structure of the choroid, important features of normal anatomy and associations with disease states are now within reach. Our methodological approach sought to optimize the information available from so-called enhanced imaging scans from currently available instruments by calculating the average choroidal thickness over the scan extension rather than using single point choroidal thickness. We chose the average thickness approach because the profile of choroidal thickness varies between individuals and because of the potential to result in measurements that are more robust. Interobserver agreement calculated after study

completion was higher for average than single point subfoveal measurements (data not shown). The wavelengths that are used in present commercial instruments are suboptimal for penetration of light into the deep choroid, leading some investigators to use wavelengths above 1000 nm, which promise greater resolution and potentially better specification of the posterior choroidal border, or CSI. While we found a high interobserver correlation in the marking of the CSI, a minority of eyes remain with a CSI that is difficult to demarcate with present instrumentation. Improved image enhancement may also offer better delineation of choroidal boundaries.

In assessing the choroidal thickness, most published investigations have reported a single location thickness, typically at the fovea, with some adding 4 additional point measures at 1.5 and 3 mm nasal and temporal to the fovea.21⁻24 However, as can be seen in our data, the choroid is thicker under the fovea than across a zone 3 mm wide centered on the fovea, as previously reported in non-glaucoma eyes.24 Whether this has functional significance in either heat dissipation or protection against light-induced damage, we cannot determine at this time. It would be ideal to have measuring scans that detail broad areas of the choroid at high resolution, including more peripheral zones, with automated demarcation of choroidal borders. This awaits further technological improvements. While there are reasonable correlations between subfoveal single point measures and average macular thickness, investigators are more likely to detect important geographic differences by thickness assessments that include broader areas of measurement.

Variations in color at the optic disc region that are generally referred to as peripapillary atrophy or crescents have been found more commonly in glaucoma eyes and develop over time as glaucoma progresses30⁻32. We found that the peripapillary choroidal thickness was related to age, axial length, CCT and DBP, but not to stage of glaucoma (suspect versus damaged eyes). Kim et al (Invest Ophthalmol Vis Sci 2010; 51: E-Abstract 2746) failed to detect an association between beta zone peripapillary atrophy and adjacent peripapillary choroidal thickness in SDOCT imaging. There are surely many alterations that lead to the appearances called peripapillary atrophy (such as lack of RPE), which would not be expressed as a change in overall choroidal thickness. For comparison, the peripapillary choroid is 250 μm thick, while the RPE is less than 20 microns high. Furthermore, our imaging was performed at an average distance of 1.77 mm from the center of the disc, which probably falls outside many crescent-shaped areas of color change.

There are potential limitations in our study. The glaucoma patients of a referral center may differ from a population-based sample of individuals with glaucoma, and we did not study a group of older adults who were not glaucoma suspects as controls, nor did we have many end-stage glaucoma eyes. Our glaucoma subgroups, particularly the PACG group, were small, so that stratification reduced the power to determine differences. To deal with this limitation we confirmed the significance of the findings using robust regression that down-weights influential observations.33 The OAGS versus OAG comparison was slightly underpowered to detect the 20%difference we proposed, but since the mean choroidal thickness was nearly identical in the two groups, a significant difference would be very unlikely even with a larger sample size. We were not able to image choroidal thickness ideally in 14% of the macular scans and 4% of the peripapillary scans with available SDOCT technology. We selected the particular SDOCT instrument used here as giving the best pilot images among 3 devices that we tested. Confirmation of our results using technology that penetrates better, such as 1060 nm wavelength SDOCT34, is likely to give a more precise estimate of the choroidal thickness.

In summary, we confirmed that increasing age and greater axial length are associated with thinner choroid, and additionally determined for the first time that diastolic perfusion

pressure and CCT also need to be considered when comparing choroidal thickness across individuals and from one time point to another. Our preliminary findings do not provide conclusive evidence that eyes with glaucoma damage have different choroidal thickness than glaucoma suspects. Nor was there significant association between degree of glaucoma injury and choroidal thickness in interocular or hemifield comparisons. Our methods provide a framework to study the role of the choroid in glaucoma and point to the need for further refinements in imaging methods.

Supplementary Material

Refer to Web version on PubMed Central for supplementary material.

Acknowledgments

Supported in part by: NIH research grant EY01765 (Core Facility Grant, Wilmer Institute), and by unrestricted gifts from the Leonard Wagner Trust, New York, NY, and Tom Forrester.

References

1. Alm, A. Ocular circulation. In: Hart, WM., Jr, editor. Adler's Physiology of the Eye. 9th ed.. St Louis, MO: Mosby; 1992. p. 198-227.
2. Smith EL III. Spectacle lenses and emmetropization: the role of optical defocus in regulating ocular development. Optom Vis Sci. 1998; 75:388–398. [PubMed: 9661208]
3. Wallman J, Winawer J. Homeostasis of eye growth and the question of myopia. Neuron. 2004; 43:447–468. [PubMed: 15312645]
4. Wildsoet CF. Active emmetropization--evidence for its existence and ramifications for clinical practice. Ophthalmic Physiol Opt. 1997; 17:279–290. [PubMed: 9390372]
5. Read SA, Collins MJ, Sander BP. Human optical axial length and defocus. Invest Ophthalmol Vis Sci. 2010; 51:6262–6269. [PubMed: 20592235]
6. Quigley HA, Friedman DS, Congdon NG. Possible mechanisms of primary angle-closure and malignant glaucoma. J Glaucoma. 2003; 12:167–180. [PubMed: 12671473]
7. Kumar RS, Quek D, Lee KY, et al. Confirmation of the presence of uveal effusion in Asian eyes with primary angle closure glaucoma: an ultrasound biomicroscopy study. Arch Ophthalmol. 2008; 126:1647–1651. [PubMed: 19064843]
8. Sakai H, Morine-Shinjyo S, Shinzato M, et al. Uveal effusion in primary angle-closure glaucoma. Ophthalmology. 2005; 112:413–419. [PubMed: 15745767]
9. Fine SL, Berger JW, Maguire MG, Ho AC. Age-related macular degeneration. N Engl J Med. 2000; 342:483–492. [PubMed: 10675430]
10. Hayreh SS. Blood supply of the optic nerve head and its role in optic atrophy, glaucoma, and oedema of the optic disc. Br J Ophthalmol. 1969; 53:721–748. [PubMed: 4982590]
11. Hayreh SS, Revie IH, Edwards J. Vasogenic origin of visual field defects and optic nerve changes in glaucoma. Br J Ophthalmol. 1970; 54:461–472. [PubMed: 4988400]
12. Kubota T, Jonas JB, Naumann GO. Decreased choroidal thickness in eyes with secondary angle closure glaucoma: an aetiological factor for deep retinal changes in glaucoma? Br J Ophthalmol. 1993; 77:430–432. [PubMed: 8343472]
13. Yin ZQ, Vaegan, Millar TJ, et al. Widespread choroidal insufficiency in primary open-angle glaucoma. J Glaucoma. 1997; 6:23–32. [PubMed: 9075077]
14. Francois J, Neetens A. Vascularity of the eye and the optic nerve in glaucoma. Arch Ophthalmol. 1964; 71:219–225. [PubMed: 14089395]
15. Gloesmann M, Hermann B, Schubert C, et al. Histologic correlation of pig retina radial stratification with ultrahigh-resolution optical coherence tomography. Invest Ophthalmol Vis Sci. 2003; 44:1696–1703. [PubMed: 12657611]
16. Chen TC, Zeng A, Sun W, et al. Spectral domain optical coherence tomography and glaucoma. Int Ophthalmol Clin. 2008 Fall;48(4):29–45. [PubMed: 18936635]

17. Nassif N, Cense B, Park BH, et al. In vivo human retinal imaging by ultrahigh-speed spectral domain optical coherence tomography. Opt Lett. 2004; 29:480–482. [PubMed: 15005199]
18. Wojtkowski M, Leitgeb R, Kowalczyk A, et al. In vivo human retinal imaging by Fourier domain optical coherence tomography. J Biomed Opt. 2002; 7:457–463. [PubMed: 12175297]
19. Spaide RF, Koizumi H, Pozzoni MC. Enhanced depth imaging spectral-domain optical coherence tomography. Am J Ophthalmol. 2008; 146:496–500. [PubMed: 18639219]
20. Esmaeelpour M, Povazay B, Hermann B, et al. Three-dimensional 1060-nm OCT: choroidal thickness maps in normal subjects and improved posterior segment visualization in cataract patients. Invest Ophthalmol Vis Sci. 2010; 51:5260–5266. [PubMed: 20445110]
21. Fujiwara T, Imamura Y, Margolis R, et al. Enhanced depth imaging optical coherence tomography of the choroid in highly myopic eyes. Am J Ophthalmol. 2009; 148:445–450. [PubMed: 19541286]
22. Ikuno Y, Kawaguchi K, Nouchi T, Yasuno Y. Choroidal thickness in healthy Japanese subjects. Invest Ophthalmol Vis Sci. 2010; 51:2173–2176. [PubMed: 19892874]
23. Ikuno Y, Tano Y. Retinal and choroidal biometry in highly myopic eyes with spectral-domain optical coherence tomography. Invest Ophthalmol Vis Sci. 2009; 50:3876–3880. [PubMed: 19279309]
24. Margolis R, Spaide RF. A pilot study of enhanced depth imaging optical coherence tomography of the choroid in normal eyes. Am J Ophthalmol. 2009; 147:811–815. [PubMed: 19232559]
25. Foster P, Buhrmann R, Quigley HA, Johnson GJ. The definition and classification of glaucoma in prevalence surveys. Br J Ophthalmol. 2002; 86:238–242. [PubMed: 11815354]
26. Akaike H. A new look at the statistical model identification. IEEE Trans Automat Contr. 1974; 19:716–723.
27. Boland MV, Quigley HA. Risk factors and open-angle glaucoma: classification and application. J Glaucoma. 2007; 16:406–418. [PubMed: 17571004]
28. Gordon MO, Beiser JA, Brandt JD, et al. Ocular Hypertension Treatment Study Group. The Ocular Hypertension Treatment Study: baseline factors that predict the onset of primary open-angle glaucoma. Arch Ophthalmol. 2002; 120:714–720. discussion 829–30. [PubMed: 12049575]
29. Spraul CW, Lang GE, Lang GK, Grossniklaus HE. Morphometric changes of the choriocapillaris and the choroidal vasculature in eyes with advanced glaucomatous changes. Vision Res. 2002; 42:923–932. [PubMed: 11927356]
30. Buus DR, Anderson DR. Peripapillary crescents and halos in normal-tension glaucoma and ocular hypertension. Ophthalmology. 1989; 96:16–19. [PubMed: 2919047]
31. Fantes FE, Anderson DR. Clinical histologic correlation of human peripapillary anatomy. Ophthalmology. 1989; 96:20–25. [PubMed: 2919048]
32. Jonas JB, Nguyen XN, Gusek GC, Naumann GO. Parapapillary chorioretinal atrophy in normal and glaucoma eyes. I. Morphometric data. Invest Ophthalmol Vis Sci. 1989; 30:908–918. [PubMed: 2722447]
33. Hamilton LC. How robust is robust regression? Stata Tech Bull. 1991 2:21–26. Available at: http://stata-press.com/journals/stbcontents/stb2.pdf.
34. Povazay B, Bizheva K, Hermann B, et al. Enhanced visualization of choroidal vessels using ultrahigh resolution ophthalmic OCT at 1050 nm. Opt Express. 2003; 11:1980–1986. [PubMed: 19466083]

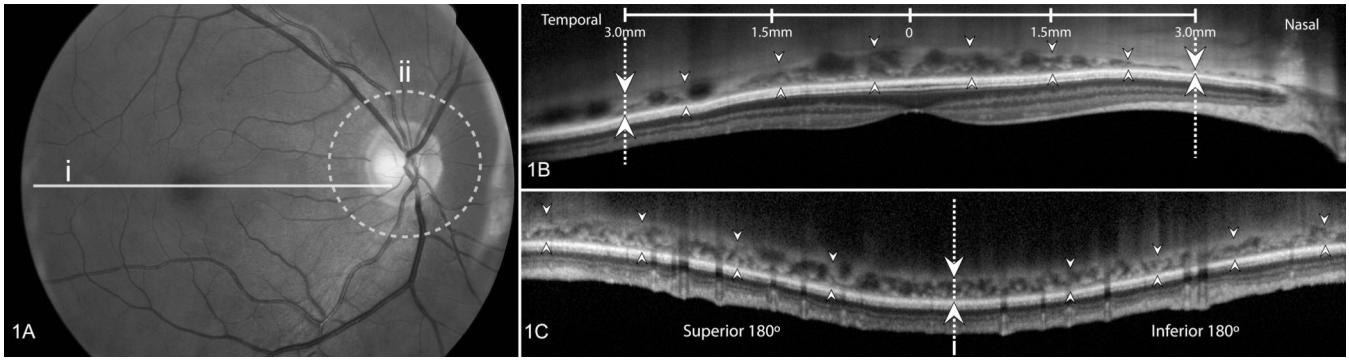

Figure 1.

Methods used for analysis of scans

Figure 1A illustrates the location of the scans used. Macular scans (solid line marked i) were 30 degrees long and centered on the fovea. Peripapillary scans (dotted circle marked ii) were taken along a circle 12 degrees in diameter, centered on the optic disc.

In Figure 1B shows a Spectral domain optical coherence tomography scan of the macula with the choroid delineated over 6 mm (from one set of dotted lines/arrows to the other) by 8 marked locations, centered on the fovea. The outer margin of the retinal pigment epithelium (RPE) was considered the anterior margin of the choroid (up-pointing arrows) and the choroidal-scleral interface (CSI) was the posterior margin of the choroid (down pointing arrows). The image was exported to ImageJ and the borders of the choroid were drawn by connecting the marked locations, leading to calculation of measured choroidal area. This area was divided by 6000 μm to estimate average macular choroidal thickness (in μm).

In Figure 1C is a scan of the peripapillary region scan in which the circular area is arrayed linearly, with the horizontal meridian at the dotted line/arrows and superior to the left and inferior to the right. As in macular scans, the RPE (up-pointing arrows) and the CSI (down-pointing arrows) delimited the choroid. After export to ImageJ for estimation of total area, this value was divided by a scan length determined for each eye by an individualized scaling factor to derive average peripapillary choroidal thickness.

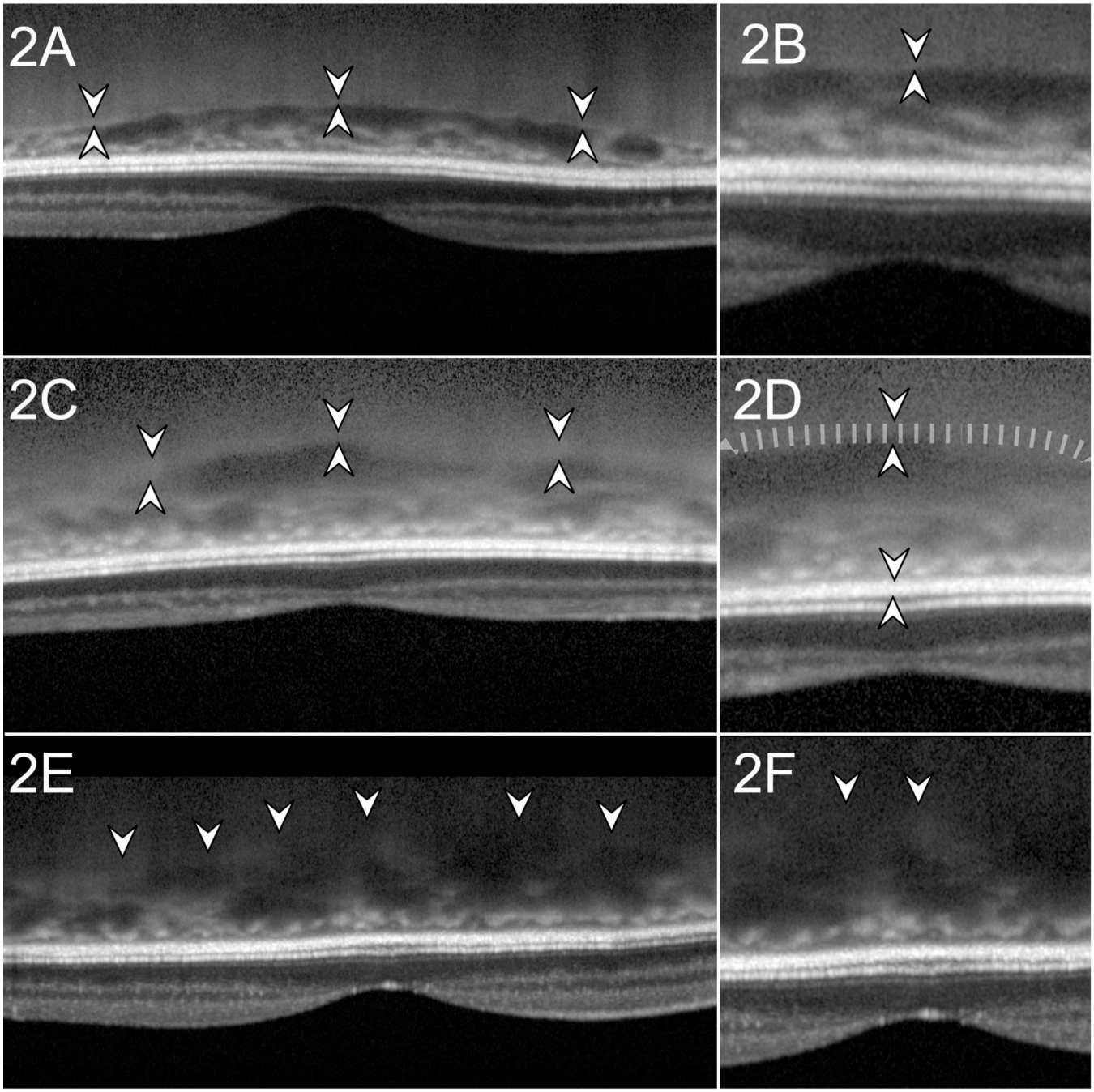

Figure 2.

Examples of scan quality, macular scans

In Figure 2A the choroidal-scleral interface (CSI) indicated by hyper-reflective line between pairs of arrowheads. Figure 2B is a magnified view of 2A and demonstrates what we classified as a good image with a hyper-reflective line whose outer border is marked as the posterior choroidal margin. Figure 2C shows a fair quality image, with thick CSI with lower contrast (between pairs of arrowheads). The CSI was considered thick when it was wider than the thickness of the retinal pigment epithelium (RPE). The outer margin of the CSI was delineated at one RPE thickness behind the inner margin of the CSI. Figure 2d is a magnified image of 2c to illustrate where the outer margin of the CSI was marked (at tip of

down-pointing smaller arrowhead). Figure 2e is an example of a poor quality image where the CSI is not distinctly seen. The posterior border of the choroid was marked as a smooth line connecting the most posterior limit of choroidal vascular spaces. Figure 2f is a magnified view of 2e.

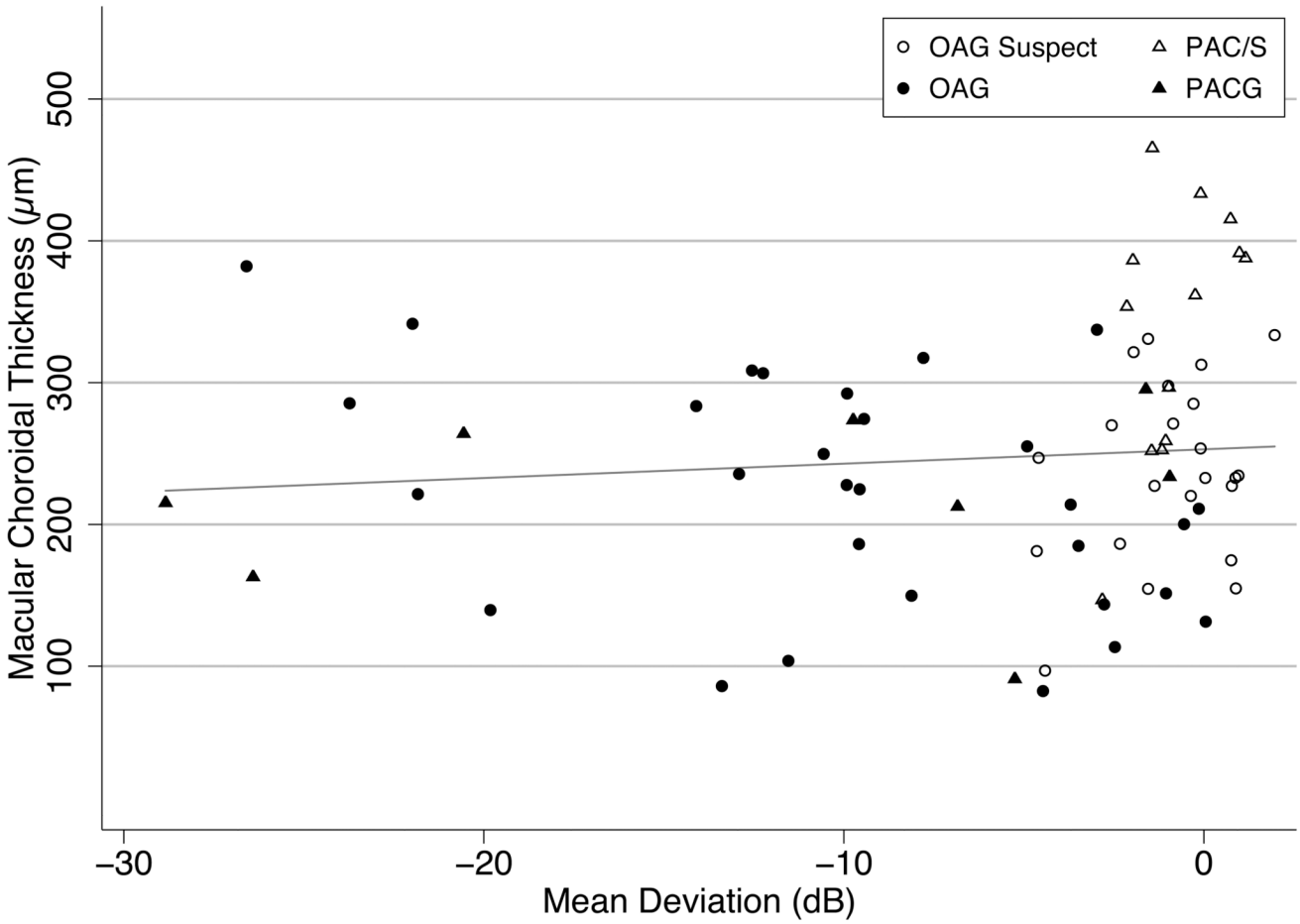

Figure 3.
Association of visual field mean deviation (MD) and choroidal thickness. The choroid is not significantly thinner at more advanced levels of damage. (Slope 1.01 μm/dB, p=0.45, R^2=0.008)
OAGS (Open Angle Glaucoma Suspect), PAC/S (Primary Angle Closure Suspect and Primary Angle Closure), OAG (Open Angle Glaucoma), PACG (Primary Angle Closure Glaucoma).

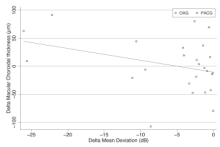

Figure 4.

For patients with macular scans of both eyes, the difference in mean deviation (worse minus better eye, X axis) is compared to the corresponding choroidal thickness difference (Y axis) There is no clear relation between thickness difference and field loss (Slope −1.32 μm/dB, p=0.2, R^2=0.03)

OAG (Open Angle Glaucoma), PACG (Primary Angle Closure Glaucoma).

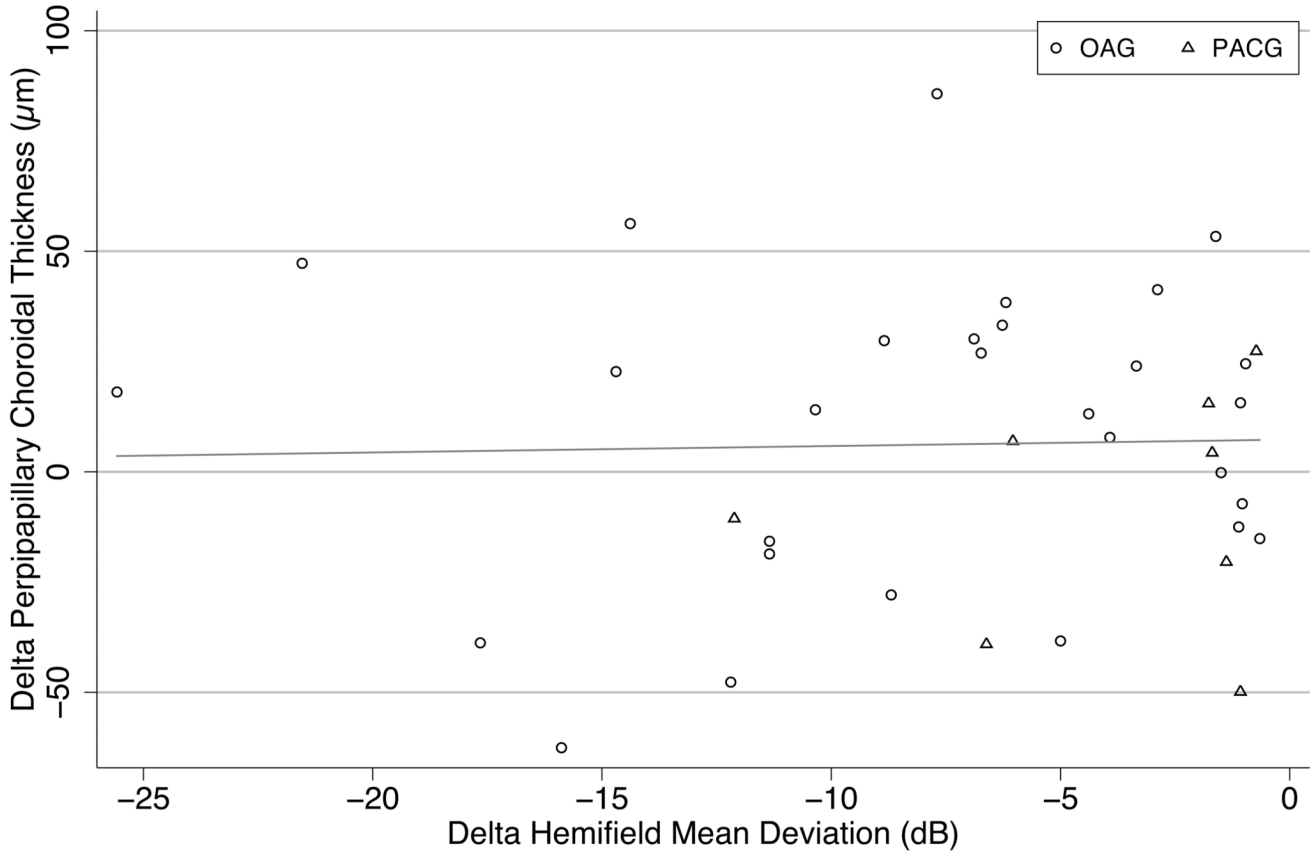

Figure 5.
Comparison of peripapillary choroidal thickness in the two hemispheres (superior versus inferior) of eyes with the hemifield mean deviation from visual field testing in the corresponding zones of the same eye (mirror image). The peripapillary choroid was not thinner in more severely damaged glaucoma hemifields. (Slope 0.005 μm/dB, p=0.87, R^2<0.001)
OAG (Open Angle Glaucoma), PACG (Primary Angle Closure Glaucoma).

Table 1

Clinical Characteristics in Study Participants

	Glaucoma Suspects		Glaucoma		Overall	
	OAGS	PAC/S	OAG	PACG		p value
N	23	13	30	8	74	
Age, years (SD)	63.1 (10.5)	58.3 (11.9)	66.5 (11.1)	63.9 (10.2)	63.7 (11.1)	0.17†
Female Gender, % (n)	52% (12)	77% (10)	57% (17)	75% (6)	45 (61%)	0.40‡
Race, % (n)						0.01‡
White	83% (19)	100% (13)	77% (23)	38% (3)	78%(58)	
Asian	4% (1)	0% (0)	0% (0)	12% (1)	3% (2)	
African-American	13% (3)	0% (0)	23% (7)	50% (4)	19% (14)	
Axial Length, mm (SD)	24.4 (1.3)	21.9 (1)	24.7 (1.8)	23.3 (1.1)	24 (1.8)	<0.001†
IOP at imaging, mmHg (SD)	16.7 (3.7)	16.1 (4)	13.3 (6.2)	16.6 (4.2)	15.2 (5.1)	0.07†
N° glaucoma meds, (SD)	0.7 (1.1)	0.2 (0.6)	1.6 (1.4)	0.4 (0.7)	0.9 (1.3)	0.002§
MD, dB (SD)	−0.9 (1.8)	−0.8 (1.2)	−9.7 (7.3)	−12.5 (11.1)	−5.7 (7.6)	<0.001§
NFL, µm (SD)	90.9 (8.3)	97.3 (13)	63.7 (12.9)	68.6 (20.7)	78.4 (19.2)	<0.001§
Highest known IOP	21.4 (7.4)	22.1 (11)	24.5 (7.2)	32.4 (14.1)	24 (9.3)	0.04§
Pseudophakia, % (n)	13% (3)	8% (1)	20% (6)	37% (3)	18% (13)	0.33‡
Previous Glaucoma Surgery, % (n)	4% (1)	0% (0)	47% (14)	75% (6)	28% (21)	<0.001‡
SBP, mmHg (SD)	131 (13.7)	126.8 (19)	131.6 (14.5)	132.6 (17)	130.6 (15.2)	0.79†
DBP, mmHg (SD)	79.7 (9.7)	77.5 (10.1)	79.3 (9.3)	78.7 (4.5)	79 (9.1)	0.91†
HR, bpm (SD)	67.8 (10.6)	69.9 (9.4)	70.1 (11.7)	74.1 (12.9)	69.7 (11)	0.62†

SD (Standard Deviation), OAGS (Open Angle Glaucoma Suspect), PAC/S (Primary Angle Closure Suspect and Primary Angle Closure), OAG (Open Angle Glaucoma), PACG (Primary Angle Closure Glaucoma), IOP (Intraocular Pressure), MD (Mean deviation), NFL (Nerve Fiber Layer Thickness), SBP (Systolic Blood Pressure), DBP (Diastolic Blood Pressure), HR (Heart Rate)

† One way analysis of variance

‡ Fischer's Exact Test

§ Kruskal Wallis non-parametric test for equality of means

Table 2

Average Macular Choroidal Thickness and Univariable Associations

	N	Beta [95% CI]	p value
Glaucoma (vs Glaucoma Suspect)	73	−54.9 [−93.6, −16.2]	0.006
Diagnosis	73		
PAC/S (vs OAGS)		100.2 [46.7, 153.7]	<0.001
OAG (vs OAGS)		−17.1 [−60.0, 25.8]	0.43
PACG (vs OAGS)		−19.9 [−83.0, 43.3]	0.53
Age (years)	73	−3.3 [−5.0, −1.6]	<0.001
Axial Length (mm)	72	−28.3 [−37.8, −18.8]	<0.001
NFL Thickness (um)	72	1.2 [0.2, 2.3]	0.02
Previous glaucoma surgery	73	−40.5 [−84.6, 3.5]	0.07
Female Sex (vs Male)	73	−21.5 [−62.9, 19.9]	0.30
Non-White Race (vs White)	73	−9.4 [−59.8, 41.1]	0.71
CCT (um)	71	−0.2 [−0.7, 0.3]	0.41
IOP at imaging (mmHg)	73	1.1 [−2.9, 5.0]	0.60
Number of glaucoma meds	73	−9.2 [−25.1, 6.7]	0.25
Visual Field MD (dB)	73	1.0 [−1.7, 3.7]	0.46
Highest known IOP (mmHg)	73	−0.8 [−3.0, 1.4]	0.45
Pseudophakia	73	44.1 [−8.2, 96.4]	0.10
SBP (mmHg)	69	−0.5 [−1.9, 0.9]	0.50
DBP (mmHg)	69	1.3 [−1.0, 3.6]	0.26
HR (bpm)	69	0.5 [−1.4, 2.4]	0.62
Systolic Ocular Perfusion Pressure (mmHg)†	69	−0.6 [−2.0, 0.8]	0.39
Mean Ocular Perfusion Pressure (mmHg)‡	69	0.4 [−1.8, 2.5]	0.73
Diastolic Ocular Perfusion Pressure (mmHg)§	69	1.0 [−1.3, 3.2]	0.40

CI (Confidence Interval), OAGS (Open Angle Glaucoma Suspect), PAC/S (Primary Angle Closure Suspect and Primary Angle Closure), OAG (Open Angle Glaucoma), PACG (Primary Angle Closure Glaucoma), CCT (Central Corneal Thickness), IOP (Intraocular Pressure), MD (Mean deviation), NFL (Nerve Fiber Layer Thickness), SBP (Systolic Blood Pressure), DBP (Diastolic Blood Pressure), HR (Heart Rate)

†Calculated as the differential pressure between SBP and IOP

‡Calculated as the differential pressure between Mean BP and IOP (In turn, Mean BP = DBP + (1/3*(SBP-DBP)))

§Calculated as the differential pressure between DBP and IOP

Table 3

Average Macular Choroidal Thickness and Stepwise Model Multivariable Associations

	Beta [95% CI]	p value
Glaucoma (vs Glaucoma Suspect)	−14.3 [−54.5, 25.8]	0.48
Female Sex (vs Male)	−31.0 [−65.7, 3.7]	0.08
Non-White Race (vs White)	−2.6 [−45.4, 40.2]	0.9
Age (years)	−3.0 [−4.4, −1.6]	<0.001
Axial Length (mm)	−26.3 [−36.1, −16.5]	<0.001
IOP (mmHg)	−1.1 [−4.5, 2.2]	0.5
CCT (um)	−0.6 [−1.0, −0.2]	0.006
Diastolic Ocular Perfusion Pressure (mmHg)†	3.0 [1.1, 4.9]	0.003
Previous Glaucoma Surgery	−45.6 [−90.6, −0.5]	0.05

CI (Confidence Interval), IOP (Intraocular Pressure), CCT (Central Corneal Thickness), DBP (Diastolic Blood Pressure), BP (Blood Pressure)

†Calculated as the differential pressure between Mean BP and IOP (Mean BP = DBP + (1/3*(SBP-DBP)))

Table 4

Relation of Choroidal Thickness to Diastolic Ocular Perfusion Pressure, Diastolic Blood Pressure, and IOP in Multivariable Regression Models[†]

	Model 1 Coeff (p value)	Model 2 Coeff (p value)	Model 3 Coeff (p value)	Model 4 Coeff (p value)
Macular Choroidal Thickness Models				
Diastolic Perfusion Pressure			2.9 (0.003)	
Diastolic Blood Pressure		2.3 (0.018)		2.86 (0.005)
IOP	−1.61 (0.323)			−3.07 (0.068)
Model Fit				
AIC[‡]	787.9	741.56	737.7	739.68
R^2	0.53	0.54	0.57	0.57
Peripapillary Choroidal Thickness Models				
Diastolic Perfusion Pressure			2.52 (0.005)	
Diastolic Blood Pressure		2.07 (0.021)		2.52 (0.007)
IOP	−1.24 (0.411)			−2.55 (0.1)
Model Fit				
AIC[‡]	777.24	730.02	726.86	728.86
R^2	0.38	0.43	0.46	0.46

[†]All models included age, sex, race, axial length, central corneal thickness and glaucoma diagnosis (glaucoma vs suspect). Coefficients reported in the table represent change in choroidal thickness per additional 1 mmHg in the predictor. (i.e., Diastolic perfusion pressure)

[‡]AIC (Akaike information criteria; lower values, indicate better model fit.)

IOP (Intraocular pressure), AIC (Akaike Information criteria), Coeff = beta coefficient value for each variable from regression models, R^2 = regression coefficient for each model.

Units for IOP, Diastolic Blood Pressure and Diastolic Perfusion Pressure are mmHg.

Table 5

Average Macular Choroidal Thickness and Stepwise Model Multivariable Associations

	Beta [95% CI]	p value
Diagnosis		
PAC/S (vs OAGS)	42.9 [−8.3, 94.1]	0.1
OAG (vs OAGS)	−14.5 [−50.4, 21.4]	0.42
PACG (vs OAGS)	−63.6 [−118.9, −8.2]	0.03
Female Sex (vs Male)	−24.1 [−57.4, 9.3]	0.15
Non-White Race (vs White)	3.6 [−37.8, 45.1]	0.86
Age (years)	−3.1 [−4.4, −1.7]	<0.001
Axial Length (mm)	−21.7 [−33.0, −10.5]	<0.001
CCT (um)	−0.6 [−1.0, −0.2]	0.005
Diastolic Perfusion Pressure (mmHg)†	2.6 [0.8, 4.4]	0.005

CI (Confidence Interval), OAGS (Open Angle Glaucoma Suspect), PAC/S (Primary Angle Closure Suspect and Primary Angle Closure), OAG (Open Angle Glaucoma), PACG (Primary Angle Closure Glaucoma), IOP (Intraocular Pressure), CCT (Central Corneal Thickness), DBP (Diastolic Blood Pressure), BP (Blood Pressure)

† Calculated as the differential pressure between Mean BP and IOP (Mean BP = DBP + (1/3*(SBP-DBP)))